J. Biochem. 2013;154(1):67–76 doi:10.1093/jb/mvt030

JB THE JOURNAL OF BIOCHEMISTRY

Spatiotemporal visualization of proHB-EGF ectodomain shedding in living cells

Received January 24, 2013; accepted March 28, 2013; published online April 18, 2013

Hirofumi Inoue[1,2,3,*], Tomohisa Sakaue[2], Takeaki Ozawa[4] and Shigeki Higashiyama[1,2]

[1]Department of Biochemistry and Molecular Genetics, Ehime University Graduate School of Medicine, Shitsukawa, Toon, Ehime 791-0295, Japan; [2]Department of Cell Growth and Tumor Regulation; [3]Ehime-Nikon Bio-Imaging Core-Laboratory, Ehime Proteo-Medicine Research Center (ProMRes), Shitsukawa, Toon, Ehime 791-0295, Japan; and [4]Department of Chemistry, School of Science, The University of Tokyo, 7-3-1 Hongo, Bunkyo-ku, Tokyo 113-0033, Japan

*Hirofumi Inoue, Department of Biochemistry and Molecular Genetics, Ehime University Graduate School of Medicine, Shitsukawa, Toon, Ehime 791-0295, Japan. Tel: +81-89-960-5254, Fax: +81-89-960-5256, email: hinoue66@m.ehime-u.ac.jp; shigeki@m.ehime-u.ac.jp

Heparin-binding epidermal growth factor (EGF)-like growth factor (HB-EGF) is a member of the EGF family, each of which is produced as a type I transmembrane precursor. The juxtamembrane domain of proHB-EGF, a precursor of HB-EGF, is cleaved by a disintegrin and metalloproteases. HB-EGF is released into the extracellular space and strongly activates EGF receptor. The relevance of better understanding proHB-EGF shedding relates to the importance of the process in the proliferation, differentiation and survival of various types of cells. Shedding of proHB-EGF is normally evaluated using an alkaline phosphatase-tagged proHB-EGF assay or a western blotting assay that involves multiple cells, which makes it difficult to observe spatiotemporal differences in the activities of the individual cells. In this study, we developed a fluorescent proHB-EGF-based metalloprotease biosensor, named Fluhemb, to visualize spatiotemporal regulation of proHB-EGF shedding in individual cells using a simple method that measures changes in fluorescence ratios. Fluhemb might be very useful for detecting the activity of proHB-EGF shedding in various types of cells under different conditions *in vitro* and *in vivo*.

Keywords: ectodomain shedding/EGF family/fluorescence bioimaging/HB-EGF/tumour.

Abbreviations: ADAM, a disintegrin and metalloprotease; EGF, epidermal growth factor; FRET, fluorescence resonance energy transfer; HB-EGF, heparin-binding EGF-like growth factor; mAG1, monomeric Azami Green 1; SDS-PAGE, sodium dodecyl sulphate–polyacrylamide gel electrophoresis; TPA, 12-O-tetradecanoylphorborl-13-acetate.

Heparin-binding epidermal growth factor (EGF)-like growth factor (HB-EGF) is a member of the EGF family, which includes EGF, amphiregulin, transforming growth factor-α, betacelulin, epiregulin, epigen and neuregulins (*1*, *2*). Expression of *HB-EGF* has been detected in most parts of the body but is found predominantly in the lungs, heart, brain, skin and skeletal muscles (*3*). HB-EGF is involved in various physiological and pathological events (*2*) such as wound healing (*4*), eyelid formation (*5*), blastocyst implantation (*6*), pulmonary hypertension (*7*), restenosis following balloon injury (*8*), atherosclerosis (*9*) and tumour progression (*10–13*). Knockout of the *HB-EGF* gene impairs the development of several neural crest cell-derived tissues, including those that define craniofacial structure, cardiac development and enteric nervous development (*14–17*). Analysis of brain-specific knockout mice also showed that the absence of HB-EGF contributes to psychiatric disorders (*18–20*).

Like other members of the EGF family, HB-EGF is initially synthesized as a transmembrane precursor, which is termed proHB-EGF (*1*, *2*). proHB-EGF is cleaved at the cell surface by proteases, such as a disintegrin and metalloproteases (ADAMs) to release HB-EGF (*21*). The process is known as ectodomain shedding (*21*). Ectodomain shedding of proHB-EGF is stimulated by various physiological or pharmacological stimuli, such as 12-O-tetradecanoylphorborl-13-estate (TPA) (*22*), calcium ionophores (*23*), G-protein coupled receptor ligands (e.g. lysophosphatidic acid (*24–27*)) and growth factors (*28*). Ectodomain shedding of proHB-EGF is essential for activation of the autocrine and paracrine growth factor activities of HB-EGF. Mice that express a non-cleavable mutant of proHB-EGF as well as *HB-EGF* null mice show severe heart failure (*29*). We also showed that the uncleavable form of proHB-EGF induces myocardial apoptosis under hypoxic conditions (*30*). On the other hand, a mutant of proHB-EGF with a truncated transmembrane domain is constitutively released from cells, and mice that express this mutant proHB-EGF demonstrate severe hyperplasia in the heart and skin (*29*). proHB-EGF shedding also affects tumour progression and has been used to develop anti-tumour drugs (*31*). These studies indicate that measurement of proHB-EGF shedding activity is critical to understanding several aspects of normal and pathological physiology.

Ectodomain shedding of proHB-EGF is usually monitored by detecting changes in the levels of truncated proHB-EGF either by western blotting or by monitoring changes in alkaline phosphatase (AP) activity in the conditioned media of AP-tagged proHB-EGF-expressing cells (*23*, *32*). Notwithstanding the value of these approaches for monitoring shedding

activities of cell populations under various conditions, it is difficult to evaluate shedding activity in individual cells *in vitro* or *in vivo*. In this study, we generated a fluorescent probe that is based on the proHB-EGF protein. Our fluorescent proHB-EGF-based metalloprotease biosensor, named Fluhemb, enables visualization of the ectodomain shedding activity of proHB-EGF in living cells. This approach might enable better understanding of the mechanism and functions of membrane-protein shedding.

Experimental Procedures

Materials

TPA was purchased from Sigma Aldrich. EGF, A23187 and GM6001 were purchased from Calbiochem. KB-R7785 was kindly provided by Carna Bioscience Inc.

Construction of Fluhemb-expressing lentivirus vector and infection of cells

To construct Fluhemb cDNA, the EGF-like region of proHB-EGF cDNA was replaced with mCherry cDNA (Invitrogen) using the In-Fusion HD cloning kit (Clontech). Monomeric Azami Green 1 (mAG1) cDNA (Medical and Biological Laboratories Co., LTD (MBL)) was inserted between the 193rd and 194th amino acid residues of proHB-EGF. This cDNA fragment, which encodes two fluorescent proteins, was inserted into the lentivirus vector pCSII-IRES2-Bsd (provided by Dr. H. Miyoshi) at the EcoRI and NotI sites. Fluhemb cDNA-containing lentivirus was produced in 293 T cells (RIKEN Bioresource Center) and was used to infect cells at a multiplicity of infection of 20.

Cell culture and assay of shedding stimulators

The human fibroblastic sarcoma cell line HT1080 and human keratinocyte cell line HaCaT were provided by the American Tissue and Cell Collection. The HT1080 cells were maintained in Eagle's minimum essential medium (Wako) containing non-essential amino acids (Life Technologies), L-glutamine (Life Technologies) and 10% foetal calf serum. HaCaT cells were cultured in Dulbecco's minimum essential medium (Wako) with L-glutamine (Life Technologies) and 10% foetal calf serum. Before stimulation with TPA or EGF, HT1080 or HaCaT cells were incubated in serum-free medium for 30 min. The time-lapse assay was performed with Biostation IM (Nikon), and the fluorescence intensity ratio, which was determined by calculating the relative intensities of the mAG1-derived signal to the mCherry-derived signal in each pixel, was analysed with NIS-Elements software.

Fluhemb localization in HT1080 cells

HT1080 cells were fixed with 4% paraformaldehyde in PBS (Nacalai Tesque) for 15 min. Fluorescent 3D images of the cells were obtained using a confocal laser microscope A1R (Nikon). The imaging data were analysed by NIS-Elements software.

Western blotting assay

The samples were subjected to sodium dodecyl sulphate–polyacrylamide gel electrophoresis (SDS-PAGE), transferred to polyvinylidene fluoride (PVDF) membranes (Bio-rad) and probed with an appropriate antibody. The antibodies used were anti-mCherry (clone: 1C51; Abcam), anti-Azami Green (MBL) and anti-beta-actin (clone: AC-15; Sigma-Aldrich; used for a loading control).

Matrigel invasion assay

Fluhemb-expressing HT1080 cells were seeded onto a single chamber of a 3D chemotaxis μ-Slide (ibidi) containing a serum-free medium. Serum-containing medium was added to another chamber. The space between the two chambers was filled with BD Matrigel (Becton, Dickinson and Company). The following day, time-lapse imaging of invading HT1080 cells migrating into Matrigel was performed every 10 min for 24 h using a Biostation IM instrument, and the fluorescence intensity ratio of mAG1 to mCherry was analysed by NIS-Elements software.

Forty-eight hours after seeding Fluhemb-expressing HT1080 cells, the cells were fixed with 4% paraformaldehyde (PFA) and stained with Alexa Fluor 647-conjugated phalloidin (Invitrogen). Fluhemb and actin were detected using a confocal laser microscope A1R, and the fluorescence intensity ratio (mAG1-derived signal relative to mCherry-derived signal) in each pixel was analysed by NIS-Elements software.

Scratch assay

Fluhemb-expressing HaCaT cells were seeded onto μ-Dish 35 mm (ibidi). Next day, the surface of the cell culture was scratched with a yellow tip, time-lapse assay was performed every 10 min for 24 h using a Biostation IM instrument and the fluorescence intensity ratio (mAG1-derived signal relative to mCherry-derived signal) in each pixel was analysed by NIS-Elements software.

Transplantation assay of Fluhemb-expressing HT1080 cells to a nude mouse

Approximately 10^6 Fluhemb-expressing HT1080 cells were transplanted subcutaneously into three 6-week-old female BALB/c nu/nu mice, and the mice were fed for 7–10 days. Following anesthetization of the mice on the day of imaging analysis using isoflurane (Mylan), fluorescent images of tumour cells obtained percutaneously by A1R and the fluorescence intensity ratio (mAG1-derived signal to mCherry-derived signal) in each pixel were analysed by NIS-Elements software.

Results

Shedding of the fluorescent proHB-EGF-based metalloprotease biosensor Fluhemb resembles the shedding of proHB-EGF

We fused the cDNA that encodes mAG1 to the cDNA that encodes the C-terminal region of proHB-EGF protein. The sequence encoding EGF region was replaced by mCherry cDNA to minimize any effects of overexpressing proHB-EGF on cell growth. The shedding biosensor named Fluhemb (Fig. 1A) was stably expressed in the HT1080 human sarcoma cell line following lentivirus infection. Confocal microscopy analysis revealed that full-length Fluhemb localized mainly in the plasma membrane, in a manner identical to that seen for wild type proHB-EGF (Fig. 1B and C). Under normal conditions, Fluhemb was expressed in HT1080 cells as a protein with a predicted size of approximately 70 kDa. However, when Fluhemb-expressing HT1080 cells (Fluhemb-HT1080 cells) were stimulated by exposure to a strong shedding inducer, TPA (50 nM), the abundance of the 70-kDa protein decreased and a 30-kDa protein that includes the mAG1 protein sequence was clearly detected (Fig. 1D). Moreover, treatment with the proHB-EGF sheddase inhibitors GM-6001 (20 μM) (*33*) and KB-R7785 (20 μM) (*34*) cancelled the effects of stimulation with TPA (Fig. 1D). These data suggest that Fluhemb was shed by activated metalloproteases such as ADAMs in the same as manner as that for proHB-EGF.

Analysis of the ratio of both fluorescent signals generated by Fluhemb indicates shedding after stimulation of individual cells with TPA

Next, we performed time-lapse imaging of Fluhemb-HT1080 after treatment with TPA. The mCherry fluorescence signal gradually decreased in a time-dependent manner after stimulation with TPA, and the fluorescence ratio of mAG1 to mCherry (mAG1/mCherry) increased (Fig. 2A–D and Supplementary Video 1). Moreover,

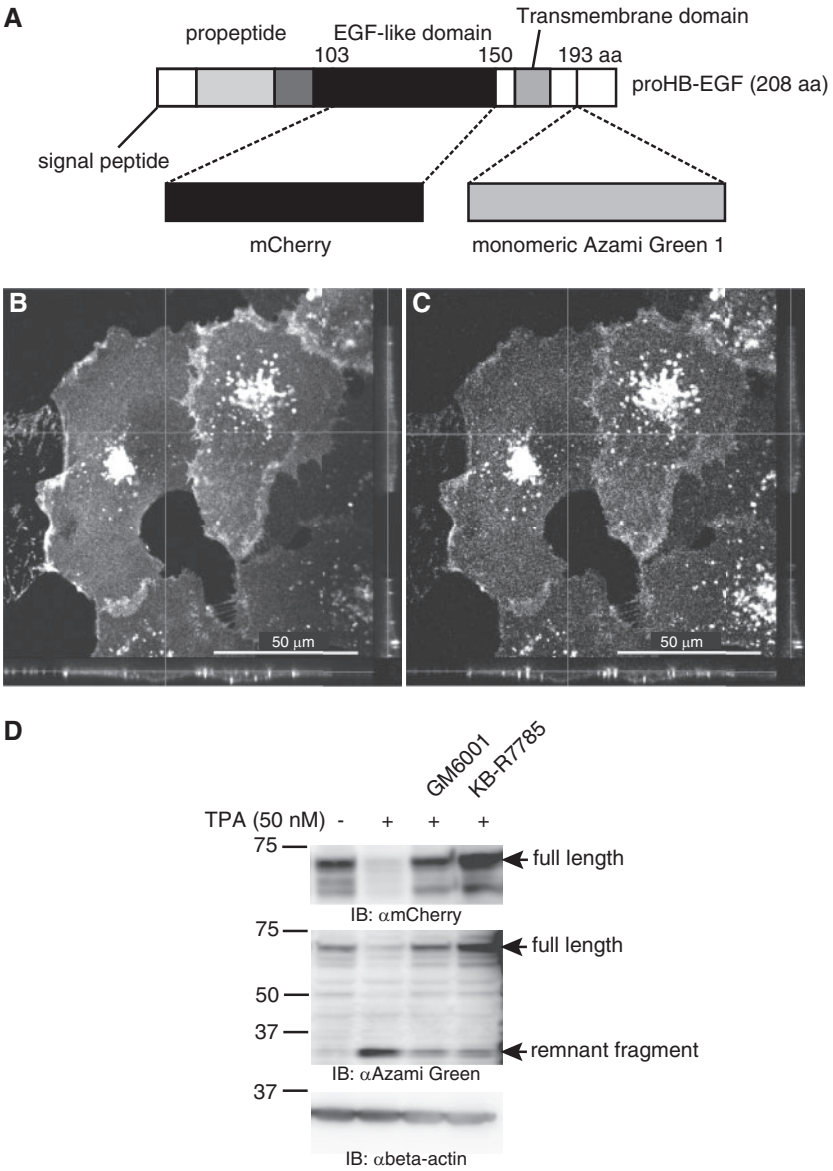

Fig. 1 Intracellular localization and biochemical characterization of the fluorescent proHB-EGF-based metalloprotease biosensor Fluhemb. (**A**) Structure of Fluhemb. (**B, C**) Confocal laser microscopic analysis of Fluhemb-HT1080 cells. The cells were fixed by 4% paraformaldehyde in PBS for 15 min and the fluorescence Fluhemb was detected using a confocal laser microscope A1R. (B) mAG1, (C) mCherry. Lower panel, X–Z section; right panel, Y–Z section. Scale bar indicates 50 μm. (**D**) After serum starvation, Fluhemb-HT1080 cells were stimulated by incubation in 50 nM TPA for 60 min. For metalloprotease inhibition, the cells were treated with 20 μM of GM6001 or KB-R7785 for 30 min before TPA stimulation. The whole-cell lysate was analysed using SDS-PAGE and western blotting. Fluhemb was detected by anti-mCherry or anti-mAG antibodies. Detection of beta-actin was used as a loading control.

treatment with either GM6001 or KB-R7785 reduced the increase in the mAG1/mCherry ratio following stimulation by TPA (Fig. 2A). This ratio seemed to be especially high near the leading edge of migrating cells (Fig. 2B and C). These data suggest that the change in the fluorescence ratio indicates shedding of proHB-EGF in individual cells.

Various stimulants of proHB-EGF shedding also increase the mAG1/mCherry ratio of Fluhemb in different cell lines

Given that proHB-EGF is shed by stimulations with various substances such as calcium ionophore and growth factors (*23*, *28*), we next attempted treatment with either a calcium ionophore or EGF to increase the mAG1/mCherry ratio. After stimulation with the calcium ionophore A23187 (20 μM), the fluorescence ratio of mAG1/mCherry increased in a time-dependent manner in both Fluhemb-HT1080 and Fluhemb-expressing HaCaT cells (Fluhemb-HaCaT cells) (Fig. 3A and B and Supplementary Videos 2 and 3). Analysis of Fluhemb fluorescence also showed that the response to A23187 was much quicker in HaCaT cells than that in HT1080 cells. Moreover, EGF stimulation (10 nM) also increased the mAG1/mCherry ratio in Fluhemb-HaCaT cells (Fig. 3C). In particular, the shedding tended to occur at the cell–cell contact regions. These data indicate that Fluhemb could be useful to evaluate the abilities of various factors that promote shedding of proHB-EGF and understand the

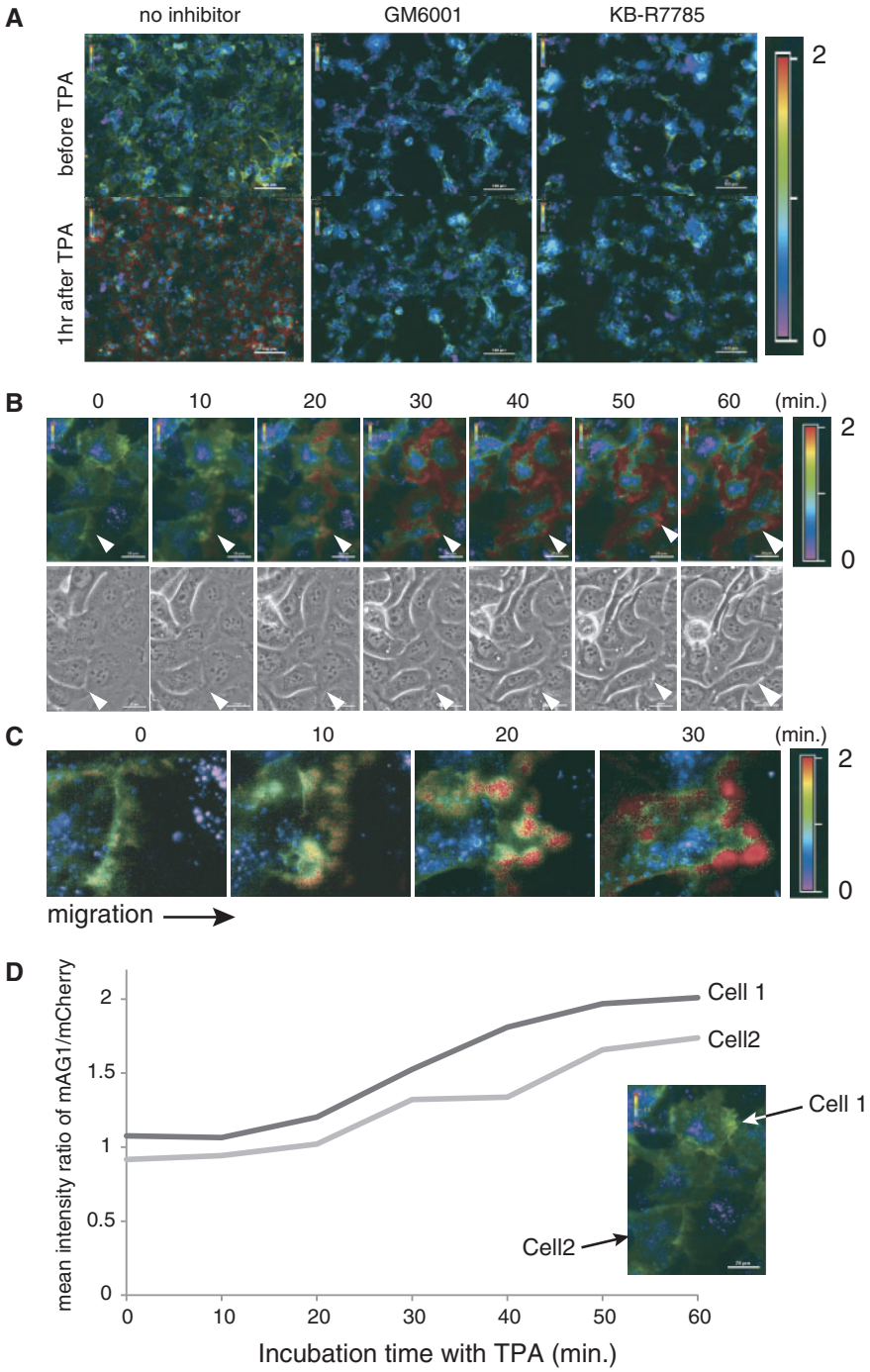

Fig. 2 Stimulation of Fluhemb-HT1080 cells with TPA. (A, B). After serum starvation, Fluhemb-HT1080 cells were stimulated by 50 nM of TPA for 60 min. For metalloprotease inhibition, the cells were treated with 20 μM of GM6001 or KB-R7785 for 30 min before TPA stimulation. Time-lapse images were obtained by Biostation IM every 1 min for 1 h. The ratio of the fluorescence intensity of mAG1 to the fluorescence intensity of mCherry was calculated by NIS-Elements, with the range of the ratio being 0–2. (B) Ratio images of the migrating cells in (A). Arrowheads indicate leading edges of the migrating cells. (**C**) High-power field images of the arrowhead indicate leading edge in (B). (**D**) Chronological changes in mean intensity ratio of mAG1/mCherry of the cells in (**B**). Rainbow-colored scales indicate the ratio of the fluorescence intensity of mAG1 to the fluorescence intensity of mCherry. Scale bars indicate 100 μm (A) and 20 μm (B).

molecular and cellular mechanism involved in the intracellular events of proHB-EGF shedding reaction.

Fluhemb reveals the local shedding of proHB-EGF in vitro

To observe proHB-EGF shedding activity under physiologically meaningful conditions, we performed two types of cell culture examinations with either Fluhemb-HT1080 or Fluhemb-HaCaT cells. First, we performed a scratch assay with Fluhemb-HaCaT cells. The mAG1/mCherry ratio was the highest in Fluhemb-HaCaT cells at the site of scratching just after scratching the surface of the cell culture (Fig. 4A, Supplementary Fig. 1 and Supplementary

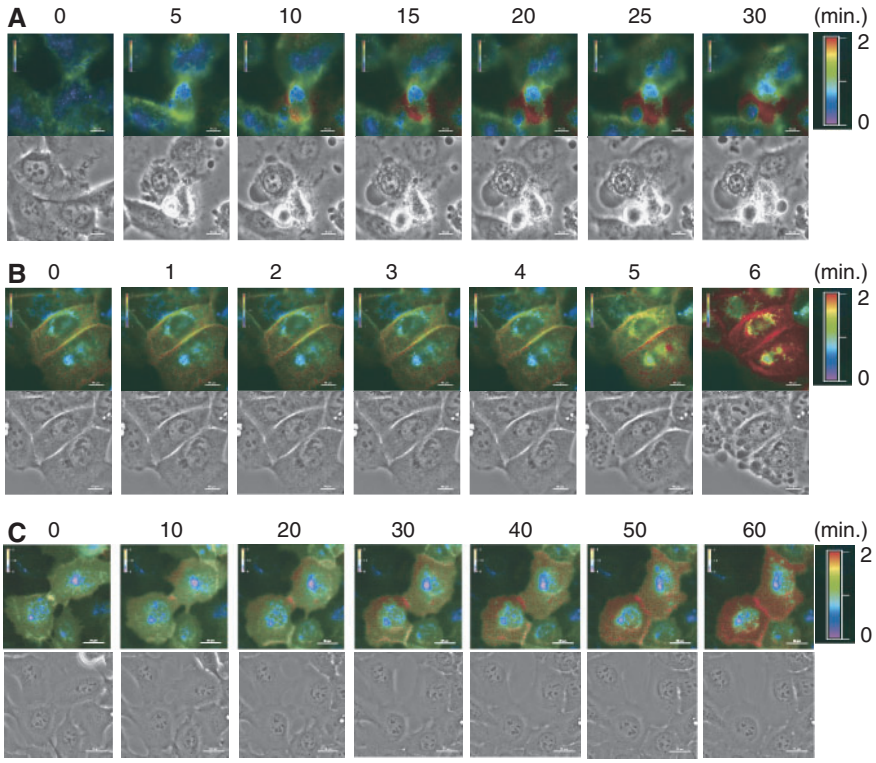

Fig. 3 The effects of shedding stimulants other than TPA on Fluhemb-HT1080 or HaCaT cells. Fluhemb-HT1080 (**A**) or Fluhemb-HaCaT (**B**) cells were treated with 20 μM of the calcium ionophore, A23187. (**C**) Fluhemb-HaCaT cells were stimulated by exposure to 10 nM of EGF after serum starvation. A time-lapse assay was performed using a Biostation IM instrument every 1 min for 1 h after the stimulation. The ratio of the fluorescence intensity of mAG1 to the fluorescence intensity of mCherry was calculated by NIS-Elements, with the range of the ratios being 0–2. Rainbow-colored scales indicate the ratio of the fluorescence intensity of mAG1 to the fluorescence intensity of mCherry. Scale bars indicate 10 μm (A and B) and 20 μm (C).

Video 4). Thereafter, the mAG1/mCherry ratio of Fluhemb decreased gradually at the edge of the scratched cellular sheet. On the other hand, the ratio of mAG1/mCherry inside the edge of the scratched cellular sheet was still kept higher than that at the edge region (Fig. 4A and Supplementary Fig. 1).

Second, we assayed the invasion of Fluhemb-expressing HT1080 cells into Matrigel. The ratio of mAG1/mCherry focally increased in the membrane protrusions of invading HT1080 cells in Matrigel (Fig. 4B and Supplementary Video 5). Moreover, the higher ratio was observed most in the actin-rich pseudopod forming region (Fig. 4C and D). The results suggest that proHB-EGF shedding might occur in a focal manner during invasion in the extracellular matrix and might be involved in invadopodia formation.

Invasive tumour cells might be detected by Fluhemb in vivo

To evaluate whether Fluhemb also works *in vivo*, Fluhemb-HT1080 cells were subcutaneously transplanted into BALB/c nu/nu female mice and observed 10 days later, using a confocal laser microscope. Most tumour cells did not show any increase in mAG1/mCherry ratio. However, local increases in this ratio were observed in several Fluhemb-HT1080 cells adjacent to blood vessels (Fig. 5A–C). These data reveal that tumour cells on blood vessels might shed more proHB-EGF than tumour cells that do not contact vessels. Taken together with the data presented in Fig. 4B, C and D, cells with a high rate of proHB-EGF shedding might be more invasive than cells with a lower rate of proHB-EGF shedding.

Discussion

Recent advances in fluorescent biosensors have facilitated analysis of the activity and distribution of enzymes in living cells (*35–37*). Biosensors of metalloprotease activities often use fluorescence resonance energy transfer (FRET) to enable visualization of their activation (*38*, *39*). The transmembrane forms of metalloproteases such as ADAMs are responsible for ectodomain shedding of members of the EGF family. However, the development of FRET-based biosensors of ectodomain shedding of members of the EGF family, including proHB-EGF, has been complicated by the need to perform such assays close to the plasma membrane, with modification of this juxtamembrane region affecting the efficiency of ectodomain shedding (*40*, *41*).

To address this challenge, we generated a proHB-EGF-based fluorescent probe in which mCherry replaced the EGF-domain and mAG1 was inserted into the cytoplasmic domain (Fig. 1A). As hoped, exposure of cells that expressed this construct to various stimuli that affect ectodomain shedding caused the expected changes of the intensities of mAG1 fluorescence

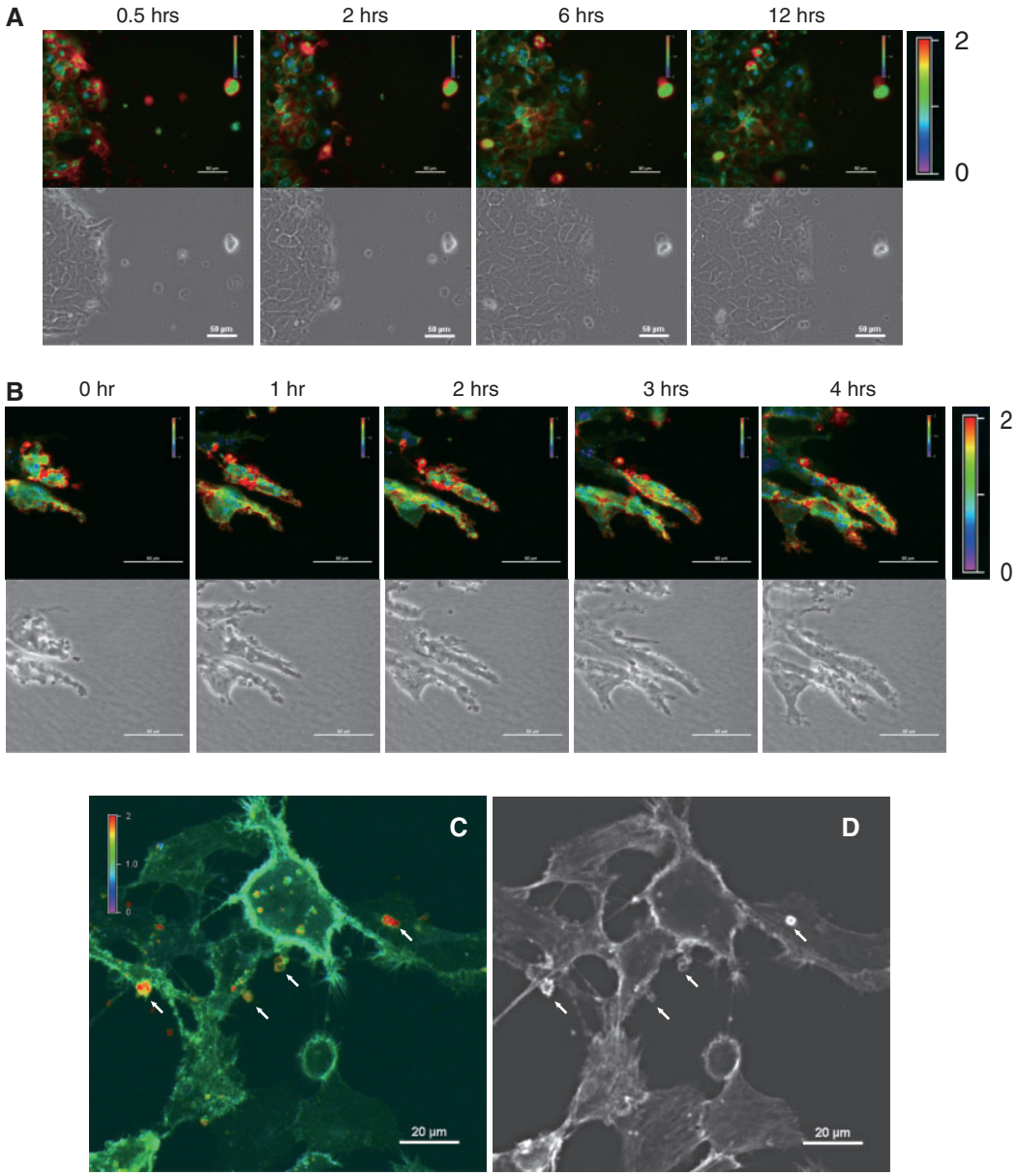

Fig. 4 Physiological stimulation of shedding to Fluhemb-expressing cells. (**A**) Fluhemb-HaCaT cells were scraped with a yellow tip, and a time-lapse assay was performed using a Biostation IM instrument. The time indicates the time elapsed since the cells were scraped. (**B–D**) Fluhemb-HT1080 cells were seeded into one chamber of a μ-slide 3D chemotaxis device, invasion into BD Matrigel was induced by adding serum-containing medium to the opposite side of the chamber, and a time-lapse assay was performed using a Biostation IM instrument. (D) Actin was detected using phalloidin conjugated to Alexa Fluor 647. Arrows indicate actin-rich pseudopods. The ratio of the fluorescence intensity of mAG1 to the fluorescence intensity of mCherry was calculated by NIS-Elements, with the range of the ratio being 0–2. Rainbow-colored scales indicate the ratio of the fluorescence intensity of mAG1 to the fluorescence intensity of mCherry. Scale bars indicate 50 μm (A and B) and 20 μm (C and D).

to mCherry fluorescence. TPA is one of the strongest inducers for proHB-EGF shedding (*22*). We first demonstrated that Fluhemb responded to TPA stimulation in HT1080 cells (Fig. 2A–D). The fluorescence intensity ratio started to change around 10 min after TPA stimulation (Supplementary Video 1). Comparison of the response of Fluhemb to TPA with previously reported rates of shedding of the proHB-EGF ectodomain shedding (*22*) suggests that changes in the fluorescence ratios of Fluhemb provide a reliable proxy for determining rates of shedding of the proHB-EGF ectodomain. Overexpression of proHB-EGF promotes cell proliferation (*42*). To minimize the effect of the proHB-EGF-based probe on the growth of cells, we replaced the EGF domain with mCherry. The data also suggest that this replacement appears to have little effect on the regulation of ectodomain shedding.

Next, we confirmed that Fluhemb worked in other cell lines when used with different stimulants of proHB-EGF shedding. The calcium ionophore A23187 stimulates proHB-EGF ectodomain shedding (*23*). Fluhemb responded to A23187 stimulation in both HT1080 and HaCaT cells (Fig. 3A and B), with differences in the

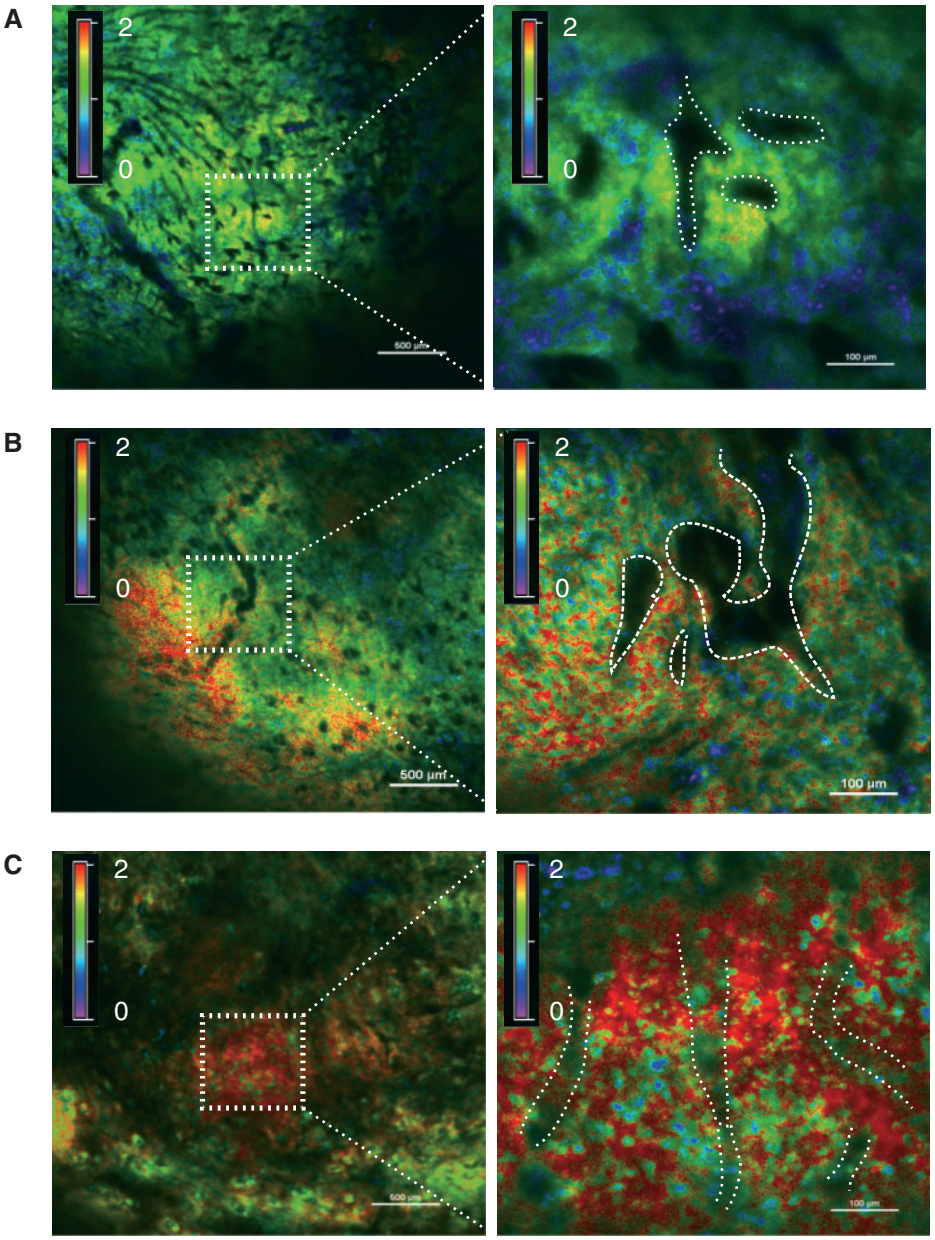

Fig. 5 Imaging of the shedding of proHB-EGF in Fluhemb-HT1080 cells in a BALB/c nu/nu mouse. Approximately 10^6 Fluhemb-HT1080 cells were subcutaneously transplanted into three 6-week-old female BALB/c nu/nu mice. Ten days after the transplantation, tumour imaging was performed using a confocal microscope A1R (Nikon). (**A**–**C**) Fluorescence ratio images of Fluhemb-HT1080 cells in each mouse. Right-side pictures show high-power field images of the dashed square region in the left-side pictures. Dendriform structure with no fluorescent signal in the low-power field and dashed area in the high-power field indicate blood vessels. Rainbow-colored scales indicate the ratio of the fluorescence intensity of mAG1 to the fluorescence intensity of mCherry. Scale bars indicate 500 μm and 100 μm in the left-side and right-side images, respectively.

speed and the pattern with which the two cell lines responded to the ionophore. We previously reported that growth factors, such as EGF or basic fibroblast growth factor, induce ectodomain shedding of proHB-EGF in keratinocytes through signalling mediated by growth factor receptors (*28*). In this experiment, Fluhemb-HaCaT cells also responded to EGF stimulation. These data indicate that Fluhemb worked in response to treatment with chemical or humoral stimulants that stimulate proHB-EGF shedding; furthermore, the findings suggested differences in proHB-EGF shedding in response to different stimulants and/or the cell types involved. The regulation of proHB-EGF shedding might differ between cell types, because proHB-EGF is shed by several ADAMs, the expression patterns of which should differ between cell types (*22*). However, there are few reports of studies that compared proHB-EGF shedding between different types of cells. Therefore, Fluhemb might become a very useful tool to identify any differences in the regulation of proHB-EGF shedding between different types of cells.

We also ascertained the response of Fluhemb to physiological stimuli. Cell motility is substantially affected by HB-EGF (*43*). During eyelid development

and healing of skin wounds, HB-EGF contributes to increased cell motility rather than promoting cell growth (*4*, *5*). In MDCK cells, expression of the uncleavable proHB-EGF mutant promoted cell–matrix and cell–cell interactions and decreased cell migration (*44*). By contrast, expression of the soluble HB-EGF mutant induced increased cell migration and decreased matrix production and cell–cell interactions (*44*). Inhibition of proHB-EGF shedding also abrogated the wound-induced activation of the EGF receptor and suppressed keratinocyte migration (*32*). The data suggest that ectodomain shedding of proHB-EGF plays a critical role in cell migration.

We also performed an *in vitro* wound-healing assay with Fluhemb-HaCaT cells. The result shown in Fig. 4A revealed that wound formation strongly induced ectodomain shedding of proHB-EGF, as reported previously (*32*). We further demonstrated local ectodomain shedding activity of proHB-EGF using a Matrigel invasion assay with Fluhemb-HT1080 cells. Shedding of proHB-EGF appeared to be prevalent in invadopodia-like protrusions of the invading cells (Fig. 4B–D). This is consistent with a report that proHB-EGF shedding contributes to the formation of invadopodia (*45*).

Finally, we visualized proHB-EGF shedding in tumour tissue *in vivo* (Fig. 5A–C). Although identification of invading tumour cells in living animals remains challenging, this method might be useful for intravital identification and tracking of invading tumour cells.

In this study, we developed a fluorescent biosensor, Fluhemb, and demonstrated its value for visualization of temporal changes in proHB-EGF shedding. Given that shedding of proHB-EGF is critical for tumour progression (*31*), Fluhemb might be used to evaluate the effects of potential anti-cancer drugs being screened for their abilities to inhibit proHB-EGF shedding. Shedding of several members of the EGF family is regulated by a range of proteases, such as ADAMs (*21*). However, the functional correlation between the shedding of each EGF family member and the activity of each particular ADAM remains unclear. Fluorescent biosensors that resemble Fluhemb but are based on different members of the EGF family might enhance our understanding of shedding in other members of the EGF family.

Supplementary Data

Supplementary Data are available at *JB* Online.

Acknowledgements

We appreciate kind gifts of lentivirus vectors from Dr. H. Miyoshi (RIKEN Bioresource Center). We are also thankful to Professor T. Imamura for the valuable advice and Dr. N. Matsushita, Mr. Y. Fujioka and Ms. M. Kurokawa for technical help.

Funding

This study was supported by a Grant-in-Aid for Scientific Research on Innovative Areas (23113512 to H.I.) from the Ministry of Education, Culture, Sports, Science and Technology of Japan.

Conflict of Interest

None declared.

References

1. Higashiyama, S., Abraham, J.A., Miller, J., Fiddes, J.C., and Klagsbrun, M. (1991) A heparin-binding growth factor secreted by macrophage-like cells that is related to EGF. *Science* **251**, 936–939
2. Raab, G. and Klagsbrun, M. (1997) Heparin-binding EGF-like growth factor. *Biochimica et Biophysica Acta*. **1333**, F179–F199
3. Abraham, J.A., Damm, D., Bajardi, A., Miller, J., Klagsbrun, M., and Ezekowitz, R.A. (1993) Heparin-binding EGF-like growth factor: characterization of rat and mouse cDNA clones, protein domain conservation across species, and transcript expression in tissues. *Biochem. Biophys. Res. Commun.* **190**, 125–133
4. Shirakata, Y., Kimura, R., Nanba, D., Iwamoto, R., Tokumaru, S., Morimoto, C., Yokota, K., Nakamura, M., Sayama, K., Mekada, E., Higashiyama, S., and Hashimoto, K. (2005) Heparin-binding EGF-like growth factor accelerates keratinocyte migration and skin wound healing. *J. Cell Sci.* **118**, 2363–2370
5. Mine, N., Iwamoto, R., and Mekada, E. (2005) HB-EGF promotes epithelial cell migration in eyelid development. *Development* **132**, 4317–4326
6. Paria, B.C., Elenius, K., Klagsbrun, M., and Dey, S.K. (1999) Heparin-binding EGF-like growth factor interacts with mouse blastocysts independently of ErbB1: a possible role for heparan sulfate proteoglycans and ErbB4 in blastocyst implantation. *Development* **126**, 1997–2005
7. Powell, P.P., Klagsbrun, M., Abraham, J.A., and Jones, R.C. (1993) Eosinophils expressing heparin-binding EGF-like growth factor mRNA localize around lung microvessels in pulmonary hypertension. *Am. J. Pathol.* **143**, 784–793
8. Igura, T., Kawata, S., Miyagawa, J., Inui, Y., Tamura, S., Fukuda, K., Isozaki, K., Yamamori, K., Taniguchi, N., Higashiyama, S., and Matsuzawa, Y. (1996) Expression of heparin-binding epidermal growth factor-like growth factor in neointimal cells induced by balloon injury in rat carotid arteries. *Arterioscler. Thromb. Vasc. Biol.* **16**, 1524–1531
9. Miyagawa, J., Higashiyama, S., Kawata, S., Inui, Y., Tamura, S., Yamamoto, K., Nishida, M., Nakamura, T., Yamashita, S., and Matsuzawa, Y. (1995) Localization of heparin-binding EGF-like growth factor in the smooth muscle cells and macrophages of human atherosclerotic plaques. *J. Clin. Investig.* **95**, 404–411
10. Jayne, D.G., Perry, S.L., Morrison, E., Farmery, S.M., and Guillou, P.J. (2000) Activated mesothelial cells produce heparin-binding growth factors: implications for tumour metastases. *Br. J. Cancer*. **82**, 1233–1238
11. Thogersen, V.B., Sorensen, B.S., Poulsen, S.S., Orntoft, T.F., Wolf, H., and Nexo, E. (2001) A subclass of HER1 ligands are prognostic markers for survival in bladder cancer patients. *Cancer Res.* **61**, 6227–6233
12. Tanaka, Y., Miyamoto, S., Suzuki, S.O., Oki, E., Yagi, H., Sonoda, K., Yamazaki, A., Mizushima, H., Maehara, Y., Mekada, E., and Nakano, H. (2005) Clinical significance of heparin-binding epidermal growth factor-like growth factor and a disintegrin and metalloprotease 17 expression in human ovarian cancer. *Clin. Cancer Res.* **11**, 4783–4792
13. Yagi, H., Miyamoto, S., Tanaka, Y., Sonoda, K., Kobayashi, H., Kishikawa, T., Iwamoto, R., Mekada,

E., and Nakano, H. (2005) Clinical significance of heparin-binding epidermal growth factor-like growth factor in peritoneal fluid of ovarian cancer. *Br. J. Cancer* **92**, 1737–1745

14. Hoshino, H., Uchida, T., Otsuki, T., Kawamoto, S., Okubo, K., Takeichi, M., and Chisaka, O. (2007) Cornichon-like protein facilitates secretion of HB-EGF and regulates proper development of cranial nerves. *Mol. Biol. Cell* **18**, 1143–1152
15. Iwamoto, R., Yamazaki, S., Asakura, M., Takashima, S., Hasuwa, H., Miyado, K., Adachi, S., Kitakaze, M., Hashimoto, K., Raab, G., Nanba, D., Higashiyama, S., Hori, M., Klagsbrun, M., and Mekada, E. (2003) Heparin-binding EGF-like growth factor and ErbB signaling is essential for heart function. *Proc. Natl Acad. U S A.* **100**, 3221–3226
16. Iwamoto, R., Mine, N., Kawaguchi, T., Minami, S., Saeki, K., and Mekada, E. (2010) HB-EGF function in cardiac valve development requires interaction with heparan sulfate proteoglycans. *Development* **137**, 2205–2214
17. Zhou, Y., James, I., and Besner, G.E. (2012) Heparin-binding epidermal growth factor-like growth factor promotes murine enteric nervous system development and enteric neural crest cell migration. *J. Pediatr. Surg.* **47**, 1865–1873
18. Oyagi, A., Moriguchi, S., Nitta, A., Murata, K., Oida, Y., Tsuruma, K., Shimazawa, M., Fukunaga, K., and Hara, H. (2011) Heparin-binding EGF-like growth factor is required for synaptic plasticity and memory formation. *Brain Res.* **1419**, 97–104
19. Oyagi, A., Morimoto, N., Hamanaka, J., Ishiguro, M., Tsuruma, K., Shimazawa, M., and Hara, H. (2011) Forebrain specific heparin-binding epidermal growth factor-like growth factor knockout mice show exacerbated ischemia and reperfusion injury. *Neuroscience* **185**, 116–124
20. Oyagi, A., Oida, Y., Kakefuda, K., Shimazawa, M., Shioda, N., Moriguchi, S., Kitaichi, K., Nanba, D., Yamaguchi, K., Furuta, Y., Fukunaga, K., Higashiyama, S., and Hara, H. (2009) Generation and characterization of conditional heparin-binding EGF-like growth factor knockout mice. *PLoS One* **4**, e7461
21. Higashiyama, S., Nanba, D., Nakayama, H., Inoue, H., and Fukuda, S. (2011) Ectodomain shedding and remnant peptide signalling of EGFRs and their ligands. *J. Biochem.* **150**, 15–22
22. Goishi, K., Higashiyama, S., Klagsbrun, M., Nakano, N., Umata, T., Ishikawa, M., Mekada, E., and Taniguchi, N. (1995) Phorbol ester induces the rapid processing of cell surface heparin-binding EGF-like growth factor: conversion from juxtacrine to paracrine growth factor activity. *Mol. Biol. Cell* **6**, 967–980
23. Dethlefsen, S.M., Raab, G., Moses, M.A., Adam, R.M., Klagsbrun, M., and Freeman, M.R. (1998) Extracellular calcium influx stimulates metalloproteinase cleavage and secretion of heparin-binding EGF-like growth factor independently of protein kinase C. *J. Cell. Biochem.* **69**, 143–153
24. Prenzel, N., Zwick, E., Daub, H., Leserer, M., Abraham, R., Wallasch, C., and Ullrich, A. (1999) EGF receptor transactivation by G-protein-coupled receptors requires metalloproteinase cleavage of proHB-EGF. *Nature* **402**, 884–888
25. Hirata, M., Umata, T., Takahashi, T., Ohnuma, M., Miura, Y., Iwamoto, R., and Mekada, E. (2001) Identification of serum factor inducing ectodomain shedding of proHB-EGF and studies of noncleavable mutants of proHB-EGF. *Biochem. Biophys. Res. Commun.* **283**, 915–922
26. Umata, T., Hirata, M., Takahashi, T., Ryu, F., Shida, S., Takahashi, Y., Tsuneoka, M., Miura, Y., Masuda, M., Horiguchi, Y., and Mekada, E. (2001) A dual signaling cascade that regulates the ectodomain shedding of heparin-binding epidermal growth factor-like growth factor. *J. Biol. Chem.* **276**, 30475–30482
27. Shiomi, T., Boudreault, F., Padem, N., Higashiyama, S., Drazen, J.M., and Tschumperlin, D.J. (2011) Lysophosphatidic acid stimulates epidermal growth factor-family ectodomain shedding and paracrine signaling from human lung fibroblasts. *Wound Repair Regen.* **19**, 229–240
28. Nanba, D., Inoue, H., Shigemi, Y., Shirakata, Y., Hashimoto, K., and Higashiyama, S. (2008) An intermediary role of proHB-EGF shedding in growth factor-induced c-Myc gene expression. *J. Cell. Physiol.* **214**, 465–473
29. Yamazaki, S., Iwamoto, R., Saeki, K., Asakura, M., Takashima, S., Yamazaki, A., Kimura, R., Mizushima, H., Moribe, H., Higashiyama, S., Endoh, M., Kaneda, Y., Takagi, S., Itami, S., Takeda, N., Yamada, G., and Mekada, E. (2003) Mice with defects in HB-EGF ectodomain shedding show severe developmental abnormalities. *J. Cell Biol.* **163**, 469–475
30. Uetani, T., Nakayama, H., Okayama, H., Okura, T., Higaki, J., Inoue, H., and Higashiyama, S. (2009) Insufficiency of pro-heparin-binding epidermal growth factor-like growth factor shedding enhances hypoxic cell death in H9c2 cardiomyoblasts via the activation of caspase-3 and c-Jun N-terminal kinase. *J. Biol. Chem.* **284**, 12399–12409
31. Miyazono, K. (2012) Ectodomain shedding of HB-EGF: a potential target for cancer therapy. *J. Biochem.* **151**, 1–3
32. Tokumaru, S., Higashiyama, S., Endo, T., Nakagawa, T., Miyagawa, J.I., Yamamori, K., Hanakawa, Y., Ohmoto, H., Yoshino, K., Shirakata, Y., Matsuzawa, Y., Hashimoto, K., and Taniguchi, N. (2000) Ectodomain shedding of epidermal growth factor receptor ligands is required for keratinocyte migration in cutaneous wound healing. *J. Cell Biol.* **151**, 209–220
33. Xu, K.P., Ding, Y., Ling, J., Dong, Z., and Yu, F.S. (2004) Wound-induced HB-EGF ectodomain shedding and EGFR activation in corneal epithelial cells. *Invest. Ophthalmol. Visual Sci.* **45**, 813–820
34. Asakura, M., Kitakaze, M., Takashima, S., Liao, Y., Ishikura, F., Yoshinaka, T., Ohmoto, H., Node, K., Yoshino, K., Ishiguro, H., Asanuma, H., Sanada, S., Matsumura, Y., Takeda, H., Beppu, S., Tada, M., Hori, M., and Higashiyama, S. (2002) Cardiac hypertrophy is inhibited by antagonism of ADAM12 processing of HB-EGF: metalloproteinase inhibitors as a new therapy. *Nature Med.* **8**, 35–40
35. Pertz, O. and Hahn, K.M. (2004) Designing biosensors for Rho family proteins—deciphering the dynamics of Rho family GTPase activation in living cells. *J. Cell Sci.* **117**, 1313–1318
36. Giepmans, B.N., Adams, S.R., Ellisman, M.H., and Tsien, R.Y. (2006) The fluorescent toolbox for assessing protein location and function. *Science* **312**, 217–224
37. Aoki, K., Kiyokawa, E., Nakamura, T., and Matsuda, M. (2008) Visualization of growth signal transduction cascades in living cells with genetically encoded probes based on Forster resonance energy transfer. *Phil. Trans. R. Soc. Lond.* **363**, 2143–2151

38. Ouyang, M., Lu, S., Li, X.Y., Xu, J., Seong, J., Giepmans, B.N., Shyy, J.Y., Weiss, S.J., and Wang, Y. (2008) Visualization of polarized membrane type 1 matrix metalloproteinase activity in live cells by fluorescence resonance energy transfer imaging. *J. Biol. Chem.* **283**, 17740–17748
39. Meyer, B.S. and Rademann, J. (2012) Extra- and intracellular imaging of human matrix metalloprotease 11 (hMMP-11) with a cell-penetrating FRET substrate. *J. Biol. Chem.* **287**, 37857–37867
40. Suzuki, M., Raab, G., Moses, M.A., Fernandez, C.A., and Klagsbrun, M. (1997) Matrix metalloproteinase-3 releases active heparin-binding EGF-like growth factor by cleavage at a specific juxtamembrane site. *J. Biol. Chem.* **272**, 31730–31737
41. Hinkle, C.L., Sunnarborg, S.W., Loiselle, D., Parker, C.E., Stevenson, M., Russell, W.E., and Lee, D.C. (2004) Selective roles for tumor necrosis factor alpha-converting enzyme/ADAM17 in the shedding of the epidermal growth factor receptor ligand family: the juxtamembrane stalk determines cleavage efficiency. *J. Biol. Chem.* **279**, 24179–24188
42. Ongusaha, P.P., Kwak, J.C., Zwible, A.J., Macip, S., Higashiyama, S., Taniguchi, N., Fang, L., and Lee, S.W. (2004) HB-EGF is a potent inducer of tumor growth and angiogenesis. *Cancer Res.* **64**, 5283–5290
43. Higashiyama, S., Abraham, J.A., and Klagsbrun, M. (1993) Heparin-binding EGF-like growth factor stimulation of smooth muscle cell migration: dependence on interactions with cell surface heparan sulfate. *J. Cell Biol.* **122**, 933–940
44. Singh, A.B., Tsukada, T., Zent, R., and Harris, R.C. (2004) Membrane-associated HB-EGF modulates HGF-induced cellular responses in MDCK cells. *J. Cell Sci.* **117**, 1365–1379
45. Hayes, K.E., Walk, E.L., Ammer, A.G., Kelley, L.C., Martin, K.H., and Weed, S.A. (2012) Ableson kinases negatively regulate invadopodia function and invasion in head and neck squamous cell carcinoma by inhibiting an HB-EGF autocrine loop. *Oncogene*, doi:10.1038/onc.2012.513